EBioMedicine 39 (2019) 118–131

Contents lists available at ScienceDirect

EBioMedicine

journal homepage: www.ebiomedicine.com

EBioMedicine
Published by THE LANCET

Research paper

Blood glutamate $EAAT_2$-cell grabbing therapy in cerebral ischemia

María Pérez-Mato [a], Ramón Iglesias-Rey [a], Alba Vieites-Prado [a], Antonio Dopico-López [a], Bárbara Argibay [a], Héctor Fernández-Susavila [a], Andrés da Silva-Candal [a], Amparo Pérez-Díaz [b], Clara Correa-Paz [a], Anne Günther [c,1], Paulo Ávila-Gómez [a], M. Isabel Loza [b], Arnd Baumann [c], José Castillo [a], Tomás Sobrino [a,*], Francisco Campos [a,*]

[a] Clinical Neurosciences Research Laboratory (LINC), Department of Neurology, Health Research Institute of Santiago de Compostela (IDIS), Clinical University Hospital, Santiago de Compostela, Spain
[b] Drug Screening Platform/Biofarma Research Group, Centro Singular de Investigación en Medicina Molecular y Enfermedades Crónicas (CIMUS), Universidade de Santiago de Compostela, Santiago de Compostela, Spain
[c] Institute of Complex Systems–Cellular Biophysics (ICS-4), Forschungszentrum Jülich, Jülich, Germany

ARTICLE INFO

Article history:
Received 20 August 2018
Received in revised form 13 November 2018
Accepted 13 November 2018
Available online 13 December 2018

Keywords:
Cell therapy
Cerebral ischemia
Excitatory amino acid transporter 2
Excitotoxic injury
Excitotoxic protection
Glutamate
Mesenchymal stem cells

ABSTRACT

Background: Excitatory amino acid transporter 2 ($EAAT_2$) plays a pivotal role in glutamate clearance in the adult brain, thereby preventing excitotoxic effects. Considering the high efficacy of $EAAT_2$ for glutamate uptake, we hypothesized that the expression of this transporter in mesenchymal stem cells (MSCs) for systemic administration could yield a cell-based glutamate-grabbing therapy, combining the intrinsic properties of these cells with excitotoxic protection.

Methods: To address this hypothesis, $EAAT_2$-encoding cDNA was introduced into MSCs and human embryonic kidney 293 cells (HEK cells) as the control cell line. $EAAT_2$ expression and functionality were evaluated by *in vitro* assays. Blood glutamate-grabbing activity was tested in healthy and ischemic rat models treated with 3×10^6 and 9×10^6 cells/animal.

Findings: The expression of $EAAT_2$ in both cell types conferred the expected glutamate-grabbing activity in *in vitro* and *in vivo* studies. The functional improvement observed in ischemic rats treated with $EAAT_2$–HEK at low dose, confirmed that this effect was indeed mediated by the glutamate-grabbing activity associated with $EAAT_2$ functionality. Unexpectedly, both cell doses of non-transfected MSCs induced higher protection than transfected $EAAT_2$–MSCs by another mechanism independent of the glutamate-grabbing capacity.

Interpretation: Although the transfection procedure most likely interferes with some of the intrinsic protective mechanisms of mesenchymal cells, the results show that the induced expression of $EAAT_2$ in cells represents a novel alternative to mitigate the excitotoxic effects of glutamate and paves the way to combine this strategy with current cell therapies for cerebral ischemia.

1. Introduction

Ischemic stroke, resulting from the interruption of blood supply to the brain, is one of the most frequent causes of morbidity and mortality worldwide [1]. During the acute phase of stroke, glutamate homeostasis is disrupted, and glutamate levels rise above physiological concentrations in the extracellular fluid. This pathological situation leads to an overstimulation of glutamate receptors, followed by the excitotoxic death of neurons [2,3]. Under physiological conditions, once glutamate is released from excitatory neurons upon an action potential, the concentration of extracellular glutamate is tightly regulated by integral membrane electrogenic transporters, known as excitatory amino acid transporters (EAATs) [3]. Five subtypes of EAATs have been identified and characterized thus far [4]. Among these, the $EAAT_2$ protein, which is mainly expressed in astroglial cells, is responsible for 90% of total glutamate uptake, thereby preventing neuronal excitotoxicity. Inside the astrocytes, glutamate is metabolized to glutamine or used for energy production. Glutamine is subsequently transferred to neurons for the replenishment of the glutamate pool *via* the glutamate–glutamine cycle [2,5,6].

The expression of $EAAT_2$ has also been described on the antiluminal surface, *i.e.*, the parenchymal side, of brain capillary endothelial cells. Here, the transporter assists in maintaining low glutamate

* Corresponding authors.
E-mail addresses: tomas.sobrino.moreiras@sergas.es (T. Sobrino), francisco.campos.perez@sergas.es (F. Campos).
[1] A.G. present address: RIKEN Center for Brain Science, Wako, Saitama 351-0198, Japan.

https://doi.org/10.1016/j.ebiom.2018.11.024

Research in context

Evidence before this study

Ischemic stroke is a major cause of morbidity and mortality worldwide. During the acute phase of stroke, glutamate homeostasis is disrupted, and glutamate levels rise above physiological concentrations in the extracellular fluid. This pathological situation leads to an overstimulation of glutamate receptors, followed by the excitotoxic death of neurons. In brain, excitatory amino acid transporters (EAATs) maintain the balance between pathological and physiological conditions by limiting the extracellular concentration of glutamate within the brain and thus preventing excitotoxic effects. Five genes have been identified in mammals encoding EAATs. Of these, $EAAT_2$ plays a pivotal role for glutamate clearance in the adult brain. The critical role of $EAAT_2$ in controlling brain glutamate homeostasis has led to the development of different therapeutic strategies to reduce the excitotoxic damage by glutamate after stroke.

Added value of the study

Mesenchymal stem cells are currently the most promising candidates for stem cell therapy against ischemic stroke owing to their intrinsic capability to secrete growth factors and immunomodulatory cytokines. Based on the high efficacy of $EAAT_2$ for glutamate uptake, we hypothesized that the induced expression of this membrane transporter in mesenchymal stem cells for systemic administration could lead to a cell-based glutamate-grabbing therapy, combining the intrinsic properties of these cells with the excitotoxic protection.

Implications of all the available evidence

Here, and for first time, we found that this cell-based therapy, using the administration of $EAAT_2$-expressing cells for ischemic lesions, could serve as a novel alternative to reduce glutamate neuronal excitotoxicity. We believe that our study makes a significant contribution to the literature because this new strategy paves the way to devise promising cell therapies for cerebral ischemia.

concentrations in the cerebral extracellular fluid, thereby establishing a brain-to-blood glutamate efflux mechanism [7,8]. When the concentration of glutamate in the extracellular fluid is elevated, glutamate is actively transported unidirectionally *via* the endothelial $EAAT_2$ into the endothelial cells, where it is accumulated until it overrides the blood concentration. Finally, glutamate is transported across the luminal membrane into the blood by facilitated diffusion [7,9,10]. Therefore, while blood glutamate may enter into endothelial cells, it can no go further, as no transport of glutamate is possible from endothelial cells into the brain [11].

The transport of glutamate by $EAAT_2$ from the extracellular fluid into either astrocytes or endothelial cells is an unfavorable and energy-consuming process. This energy is provided by a coupled co-transport of three sodium ions, one proton, and one glutamate molecule in the counter-transport of one potassium ion. Notably, the transporters also function as anion-selective channels [4].

The critical role of $EAAT_2$ in controlling brain glutamate homeostasis has led to the development of different therapeutic strategies to reduce the excitotoxic damage by glutamate after stroke. β-lactam antibiotics such as ceftriaxone have been described to be transcriptional activators of $EAAT_2$. Due to the increase in $EAAT_2$ gene expression and transport activity, treatment with antibiotics results in facilitated glutamate uptake by astroglial cells and thus neuronal protection against ischemic insult [3,5].

The brain-to-blood glutamate efflux mechanism mediated by endothelial $EAAT_2$ has also permitted the development of a new generation of protective drugs against ischemic glutamate toxicity, namely, blood glutamate-grabbers. These blood glutamate-grabbers can metabolize and thus reduce the glutamate concentration in the blood. This leads to a larger glutamate gradient between the brain and blood, facilitating the efflux of extracellular brain glutamate *via* endothelial cells into the blood. In the blood, glutamate is metabolized by the activity of glutamate oxaloacetate transaminase 1 (GOT1), which catalyzes the transformation of oxaloacetate and glutamate into aspartate and α-ketoglutarate. Thus, the administration of both oxaloacetate and/or recombinant GOT1 (rGOT1) in ischemic animal models reduces glutamate in both the blood and the brain, which improves functional recovery after an ischemic lesion [9,12–17]. The protective efficacy of this strategy has been shown in different types of ischemic animal models and has been validated in humans by pharmacological [18] and non-pharmacological approaches such as peritoneal dialysis [19]. It has also been tested in other pathological models associated with an increase in glutamate in the brain, such as traumatic brain injury [20], subarachnoid hemorrhage [21], glioma [22], amyotrophic lateral sclerosis [23], or Alzheimer's disease [24], with successful results.

On the basis of the substantial increase in glutamate uptake in astrocytes by the overexpression of $EAAT_2$ and the promising efficacy of the brain-to-blood glutamate efflux mechanism [3,9], we hypothesized that combining $EAAT_2$ expression in therapeutic cells for systemic administration might accomplish an alternative cell-based glutamate-grabbing therapy, *i.e.*, by combining certain intrinsic cell properties with excitotoxic protection.

Therefore, $EAAT_2$-encoding cDNA was introduced and functionally expressed in mesenchymal stem cells (MSCs), which are among the best candidates for stem cell therapy for ischemic stroke owing to their ability to release growth factors, as well as their immunomodulatory capacities [25]. For independent control experiments, $EAAT_2$ was introduced into human embryonic kidney 293 (HEK 293) cells, which do not interfere with ischemic damage *per se*. The expression and functionality of $EAAT_2$ in both cell types were evaluated by several *in vitro* assays, and the blood glutamate-grabbing activity was tested in ischemic animals and compared with that resulting from oxaloacetate treatment.

2. Experimental procedures

2.1. Culture of MSCs

Commercially available rat MSCs (Trevigen; Cultrex, Gaithersburg, MD, USA) were cultured in a medium consisting of Iscove's modified Dulbecco's medium (Gibco-Invitrogen, Waltham, MA, USA) supplemented with 10% fetal bovine serum (FBS; Gibco-Invitrogen), 10% horse serum (Gibco-Invitrogen), 1% penicillin-streptomycin (PS; Gibco-Invitrogen), and 1% antimycotic solution (amphotericin; Sigma-Aldrich, St. Louis, MO, USA). The cells were maintained at 37 °C in a humidified atmosphere and 5% CO_2.

2.2. Culture of HEK 293 cells

HEK 293 cells obtained from ECACC (Sigma-Aldrich, Taufkirchen, Germany) were cultured in minimum essential medium (MEM) GlutaMAX I (Gibco-Invitrogen) supplemented with 10% FBS, 1% MEM non-essential amino acids (Gibco-Invitrogen), 1% PS, and 1% amphotericin. The cells were maintained at 37 °C in a humidified atmosphere and 5% CO_2.

2.3. Transfection and expression of $EAAT_2$ in cell lines

To functionally express $EAAT_2$ in MSCs and HEK cells, we generated recombinant adeno-associated virus serotype 2 (rAAV2) harboring the coding sequence for yellow-fluorescent protein (YFP) N-terminally fused in-frame to the coding sequence of $EAAT_2$. We observed good transduction rates in HEK cells (≥50%) but rather low efficiencies in MSCs (approximately 5–10%). Changing the AAV serotype from AAV2 to AAV6 did not overcome the low transduction rate in MSCs. Therefore, we changed the expression strategy and used a plasmid containing the N-terminally YFP-tagged $EAAT_2$ cDNA (pRcCMVmYFPEAAT$_2$) for cell transfection (see Fig. S1).

YFP-$EAAT_2$ expression in MSCs was achieved using an electroporation method as previously described [26]. For electroporation, cells were resuspended in Human MSC Nucleofector Solution (Amaxa Biosystems, Cologne, Germany) at a concentration of 1×10^6 cells/100 μL. The cell suspension was mixed with 4 μg endotoxin-free plasmid DNA in a sterile electroporation cuvette (Amaxa Biosystems) and electroporated with the U-23 program. After electroporation, the cells were incubated for 5 min at RT and then transferred to culture dishes pretreated with poly-D-lysine (Sigma-Aldrich) containing prewarmed growth medium. After 24 h, the medium was changed to remove debris and dead cells.

For the expression of YFP-$EAAT_2$ in HEK cells, the plasmid was transfected using calcium phosphate co-precipitation according to the protocol described by Chen and Okayama [27]. Since the plasmid contains a neomycin resistance gene, stably transfected cells were selected in medium containing 1.2 mg/mL geneticin (G-418; Gibco-Invitrogen). Antibiotic-resistant colonies were isolated and maintained in culture medium supplemented with 1 mg/mL G-418 and examined for homogeneity based on YFP fluorescence.

Viral transduction and plasmid transfection methods are described in detail in the Supporting Information.

2.4. Assessment of YFP-$EAAT_2$ expression in MSCs and HEK cells

The expression of YFP-tagged $EAAT_2$ was evaluated and quantified at 24, 48, and 72 h post transfection using fluorescence microscopy and flow cytometry, respectively. Fluorescence microscopy was performed with an Olympus microscope, model IX51 (Olympus, Shinjuku, Tokyo, Japan). In the flow cytometry analysis, 30,000 gated events (cells) were collected. A cell was considered positive for YFP expression when its fluorescence was higher than the threshold settings of the non-transfected control sample. The percentage of YFP-fluorescent cells was calculated with respect to the total number of cells. Flow cytometry analysis was performed with a FACSAria II analyzer (BD Biosciences, Franklin Lakes, NJ, USA), and data were analyzed with the FACSDiva software program (BD Biosciences).

2.5. Immunostaining of $EAAT_2$ in transfected MSCs and HEK cells

Cells were grown on glass coverslips, which were previously treated with 0.1 mg/mL poly-D-lysine hydrobromide (Sigma-Aldrich). Cells were rinsed with phosphate buffered saline (PBS) and fixed in 4% (*w*/*v*) paraformaldehyde (PFA) solution (Thermo Fisher Scientific, Waltham, MA, USA) for 5 min at room temperature (RT), and then washed thrice with PBS. Non-specific binding sites were blocked with 0.5% (*w*/*v*) bovine serum albumin (BSA) (GE Healthcare, Chicago, IL, USA) solution for 30 min at RT. Cells were incubated with anti-$EAAT_2$ antibodies (Millipore, Burlington, MA, USA) diluted 1:100 in 0.5% (w/v) BSA in PBS solution for 24 h at 4 °C. Cells were washed thrice with PBS at RT and incubated with a biotinylated horse anti-mouse IgG antibody, rat adsorbed (dilution 1:200; Vector Laboratories, Burlingame, CA, USA), for 1 h at RT, followed by a second incubation with a 1:100 dilution of avidin–biotin (Vector Laboratories) for 30 min. Once washed, the samples were incubated with DyLight 594 streptavidin (diluted 1:500 in PBS; Vector Laboratories) for 30 min at RT, followed by a last incubation step with Hoechst stain (diluted 1:6000; Invitrogen) for 5 min. Fluorescence was analyzed with a confocal microscope (LEICA AOBS-SP5X; Leica, Wetzlar, Germany).

2.6. Characterization of transfected MSCs

Flow cytometry, tube formation assay, and growth factor release analysis were performed to verify that the transfected MSCs maintained their intrinsic phenotype properties.

Flow cytometry analysis: MSCs were harvested using trypsinization, washed, and resuspended in PBS. The typical phenotype of MSCs is $CD90^+/CD73^+/CD45^-$. Cells were stained with CD90-PerCP-Cy5 (clone OX-7; 5 μL/1 × 10^5 cells; Immunostep, Salamanca, Spain), CD73-APC (clone 5F/B9; 1 μL/1 × 10^5 cells; Immunostep), and CD45-PE (clone OX-22; 2.5 μL/1 × 10^5 cells; BD Biosciences) antibodies. After immunostaining, the cells were suspended in 200 μL PBS for subsequent analysis. The analysis was performed using a BD FACSAria II analyzer (BD Biosciences). Unlabeled MSCs were used as a negative control. Dead cells and debris were excluded based on side and forward scatter profiles (SSC and FSC, respectively). Appropriate isotype control antibodies, "fluorescence minus one" staining, and staining of negative populations were used to establish compensation parameters and sorting gates. Data were analyzed using FACSDiva software (BD Biosciences).

Tube formation assay: Matrigel-reduced growth factor (BD Biosciences) was used as a substrate to assess tube formation capacity as an *in vitro* measurement of functional angiogenesis in non-transfected MSCs ($MSCs^-$) and transfected MSCs ($MSCs^+$). Standard 24-well plates were coated with 200 μL cold matrigel. MSCs were added onto matrigel-coated wells at 1×10^4 cells per well in growth medium. Cells were incubated for 12 h at 37 °C and 5% CO_2 in a humidified atmosphere. After medium removal, cells were fixed in 4% (*w*/*v*) PFA in PBS, and images were captured using an inverted microscope (Olympus IX51). Tube formation was assessed by counting the number of circular structures (rings) and branching points (tube joints). Five random fields were examined for each well.

Vascular endothelial growth factor (VEGF) analysis in cell culture supernatants: The levels of VEGF in $MSCs^-$ and $MSCs^+$ were measured with a Quantikine VEGF ELISA kit (R&D Systems, Minneapolis, MN, USA) following the manufacturer's instructions. The detection limit was 31.2 pg/mL (VEGF ELISA kit), and values were corrected for the amount of total cell protein calculated by the Bradford assay (Bio-Rad, Hercules, CA, USA).

2.7. Analysis of interleukin-6 production in MSCs after transfection and lipopolysaccharide treatment

Non-electroporated and electroporated MSCs (without plasmid and with control and $EAAT_2$-plasmid), were seeded in culture dishes pretreated with poly-D-lysine (Sigma-Aldrich). After 24 h, the medium was removed, and it was replaced with fresh medium containing lipopolysaccharide (LPS) (1 μg/mL; Sigma-Aldrich) [28]. The supernatants were harvested by centrifugation at 3000 rpm for 20 min and stored at −80 °C until further use. The levels of interleukin-6 (IL-6) were measured with an IL-6 ELISA kit (Abbexa, Cambridge, UK) following the manufacturer's instructions. The detection limit was 3.3 pg/mL (IL-6 ELISA kit), and values were corrected for the amount of total cell protein calculated by the Bradford assay (Bio-Rad). The plasmid encoding the fluorescent protein eGFP (pmaxGFP) was used as the control (VPE 1001; Lonza, Basel, Switzerland).

2.8. Glutamate uptake assay

The uptake of radiolabeled glutamate was assessed using a competition assay. Transfected cells (HEK^+ cells and $MSCs^+$) expressing $EAAT_2$

were plated in triplicate (1.5×10^5 cells per well) on 24-well tissue culture plates pre-treated with poly-D-lysine hydrobromide (Sigma-Aldrich). Non-transfected cells (HEK^- and $MSCs^-$) were used as the negative control, and astrocytes were employed as the positive control. After 24 h, the medium was aspirated, and cells were washed thrice with 250 μL PBS at RT. Then, 500 μL PBS supplemented with 13 nM L-[^{3}H]glutamate (1 μCi/μL; Sigma-Aldrich; specific activity = 51.1 Ci/mmol) and increasing concentrations (10^{-8}–10^{-3} M) of non-labeled glutamate were added. Non-labeled glutamate was added to each well, and the plate was incubated at 37 °C for 10 min. The plates were placed on ice, and cells were washed thrice with ice-cold PBS. Cells were lysed with 200 μL 0.2 M NaOH for 4 h at 4 °C under continuous shaking. From each lysate, 50 μL was transferred to a 96-well multiplex plate, and 150 μL Optiphase buffer was added to each well. The multiplex plate was shaken for 30 min at RT. Radioactivity was determined by scintillation counting (PerkinElmer, Waltham, MA, USA), and the total protein content in lysates was determined by the Bradford assay (Bio-Rad). The results were expressed in radioactive disintegrations per minute per microgram of cellular protein.

To determine the specificity of glutamate uptake, two inhibitors of $EAAT_2$—dihydrokainate (DHK) and DL-threo-beta-benzyloxyaspartate (TBOA) (Tocris, Bioscience, Avonmouth, Bristol, UK)—were employed. Both inhibitors were used individually and jointly at concentrations of 300 μM (DHK) and 500 μM (TBOA) based on previous studies [8].

2.9. In vitro toxicity test

Cell death was evaluated by measuring the leakage of lactate dehydrogenase (LDH) into the medium, as well as the cell proliferation rate. Basal LDH and LDH release at 24, 48, and 72 h after transfection were measured in control and transfected cells. A negative control of lysed cells was also included (death control), according to the manufacturer's protocol. After centrifugation (7 min, 3000 rpm) of the supernatants, 75 μL was transferred in a 96-well plate and mixed with 150 μL LDH reagents following the manufacturer's protocol (Lactate Dehydrogenase Assay Kit; Sigma-Aldrich). After 20 min incubation at RT, the LDH activity was determined at 490 nm using a spectrophotometer (Synergy 2; BioTek, Winooski, VT, USA).

2.10. Proliferation rate

To determine the proliferation rate, the total cell number was examined using a Neubauer chamber. The number of viable cells was determined using the Trypan blue exclusion assay.

2.11. Experimental animals

Experimental protocols were approved by the local Animal Care Committee according to the European Union (EU) rules (86/609/CEE, 2003/65/CE, and 2010/63/EU). Male Wistar rats (Harlan Laboratories, Barcelona, Spain) weighing 300 ± 25 g were used. The animals were kept at controlled conditions of temperature (22 °C ± 1 °C) and humidity (60% ± 5%) with a 12/12 h light/dark cycle for a week prior to surgery and up to 14 days after surgery. Rats had access to food and water *ad libitum*. Anesthesia was induced by the inhalation of 5% sevoflurane in a nitrous oxide/oxygen mixture (70/30). Rectal temperature was monitored and maintained at 37 °C ± 0.5 °C by using a feedback-controlled heating system. Glucose levels were found to be 100–180 mg/dL before surgery. At the end of the procedures, rats were sacrificed under deep anesthesia (8% sevoflurane).

2.12. Surgical procedures

Transient focal ischemia was induced in rats by transient middle cerebral artery occlusion (MCAO) following previously described surgical procedures [12,29]. According to our reported protocol [29], the following exclusion criteria were used: (i) <70% reduction in relative cerebral blood flow during artery occlusion; (ii) arterial malformations, as determined by magnetic resonance angiography; (iii) baseline lesion volume of <25% or > 45% with respect to the ipsilateral hemisphere, as measured using apparent diffusion coefficient (ADC) maps; and (iv) absence of reperfusion or prolonged reperfusion (>10 min until achievement of at least 50% of the baseline cerebral blood flow) after filament removal. All excluded or deceased animals were replaced until the total number of animals indicated for each group was attained. Additional details of the surgical procedures are indicated in the Supporting Information.

2.13. In vivo experimental protocol

This study was divided into two steps: a dose-response study and a protective study.

Dose-response study: different doses of $MSCs^+$ and HEK^+ cells were evaluated for blood glutamate reduction after i.v. administration and compared with the same dose of non-transfected cells ($MSCs^-$ and HEK^-) with an oxaloacetate-treated group and a control group treated with saline.

Protective study: To evaluate the protective effect of $MSCs^+$ and HEK^+ cells against ischemic lesions, transfected cells were tested in ischemic animal models, and their effect on blood glutamate reduction, infarct volume, and functional recovery was compared with the effect of the administration of non-transfected cells ($MSCs^-$ and HEK^-) with oxaloacetate and with that of a control group treated with saline.

The experimental groups, glutamate and IL-6 analysis in blood samples and functional test are summarized in the Supporting Information.

2.14. Magnetic resonance studies

All magnetic resonance imaging (MRI) studies were conducted on a 9.4 T horizontal bore magnet (Bruker BioSpin, Ettlingen, Germany) according to a previously described protocol [16,29,30]. MRI post-processing was performed using ImageJ software (https://imagej.nih.gov/ij/). Additional details about MRI sequences and data analysis are described in the Supporting Information.

2.15. Brain histological analysis

Animals were sacrificed 14 days after surgical treatment, and brain tissue was processed for histological analysis. Neuronal nuclear protein (NeuN) labeling was combined with labeling of the astrocyte marker; glial fibrillary acidic protein (GFAP). GFAP-positive and NeuN-positive cells and nuclei were counted manually in Image J software. Detailed protocols are described in the online Supporting Information.

2.16. Statistical analysis

All data are presented as the mean ± standard deviation of the mean (mean ± SD). One-way or two-way analysis of variance (ANOVA) followed by post-hoc Bonferroni evaluation was used for multiple groups to determine significant differences. Student's *t*-test was used to test the differences between two groups. Statistical significance was set at $^*p < 0.05$, $^{**}p < 0.01$, and $^{***}p < 0.001$. The statistical analysis was conducted using GraphPad Prism v.6.05 for Windows (GraphPad, La Jolla, CA, USA).

3. Results

3.1. $EAAT_2$ expression in MSCs and HEK 293 cells

$EAAT_2$ was initially expressed in MSCs and HEK 293 cells by rAAV2 transduction. However, we did not achieve sufficient transduction rates (≥30%) in MSCs (see supplemental results and Figs. S2 and S3),

which led us to change the heterologous expression strategy. For MSCs, three different transfection methods were consecutively tested: calcium phosphate co-precipitation, lipofectamine transfection, and electroporation (With electroporation, we obtained successful and reliable expression rates of ≥60%).

Since the construct coded for an N-terminally YFP-tagged $EAAT_2$ protein, successful expression of the fusion protein in MSCs ($MSCs^+$) could be monitored by confocal microscopy (Fig. 1A). Using flow cytometry analysis, maximum cells (≥60%) expressing the YFP-$EAAT_2$ protein were observed 48 h after transfection (Fig. 1B). No YFP expression was detected in MSCs electroporated without the plasmid ($MSCs^-$). To evaluate the potential cell damage induced by electroporation, MSC proliferation and toxicity rates were determined. Notably, electroporation caused a significant ($p < 0.05$) reduction in MSC^+ proliferation 24 and 48 h after transfection compared to $MSCs^-$. This effect, however, was not observed 72 h after electroporation (Fig. 1C). Toxicity analysis was performed by LDH assay. There were no significant differences between $MSCs^+$ and $MSCs^-$ (Fig. 1C, lower panel). Finally, confocal microscopy confirmed the expression of YFP-$EAAT_2$ in $MSCs^+$ (Fig. 1D, E), with a preferential localization in the cell membrane (Fig. 1D).

In addition to MSCs, HEK 293 cells were transfected with the same plasmid using the calcium phosphate co-precipitation technique [27]. Since the plasmid harbors a neomycin resistance gene, stably transfected cell clones constitutively expressing YFP-$EAAT_2$ (HEK^+) were selected and maintained in the presence of the antibiotic geneticin (G418). The expression of the construct in HEK^+ cells was inspected by confocal microscopy (Fig. 2A). Flow cytometry showed that the initial transfection efficiency was ≥50% (Fig. 2B). In contrast to electroporation used for MSCs, calcium phosphate co-precipitation did not have an impact on the proliferation rate or toxicity of cells transfected without (HEK^-) or with the plasmid (HEK^+) (Fig. 2C). Selection with geneticin resulted in the isolation of cell clones that homogeneously (≥95%) expressed the construct (Fig. 2D, E).

Summary of the procedures used to induce the expression of $EAAT_2$ in MSCs and in HEK cells is represented in Fig. S4.

3.2. Functional analysis of $EAAT_2$ in $MSCs^+$ and HEK^+ cells

To evaluate the functionality of $EAAT_2$ expressed in both cell types, uptake assays with [^{3}H]glutamate were conducted in $MSCs^+$ and HEK^+ cells. For the control, assays were also performed in primary astrocytes that are known to express $EAAT_2$ endogenously [3]. The uptake of [^{3}H]glutamate (13 nM) in astrocytes was determined in the presence of increasing concentrations of unlabeled glutamate (10^{-8}–10^{-3} M). The uptake of [^{3}H]glutamate was significantly reduced (EC_{50} = 19 μM), and the concentration-response curve saturated at glutamate concentrations of ≥5×10^{-4} M. The uptake of [^{3}H]glutamate was also measured in the presence of specific inhibitors of glial $EAAT_2$ activity [8,31]: TBOA and DHK. We found that 500 μM DHK and 300 μM TBOA efficiently inhibited the [^{3}H]glutamate uptake in astrocytes (see Fig. S5).

The incubation of $MSCs^+$ with 13 nM [^{3}H]glutamate in the presence of increasing amounts of non-labeled glutamate (10^{-8}–10^{-3} M) showed specific glutamate uptake. The competitive effect was saturated at concentrations of ≥5×10^{-4} M of non-labeled glutamate, and the EC_{50} calculated from the concentration-response curve was 65 μM. In $MSCs^-$, no specific uptake of [^{3}H]glutamate was detected (Fig. 3A). Glutamate uptake in $MSCs^+$ was abolished when TBOA (300 μM) and DHK (500 μM) were included in the assay either in combination (Fig. 3B) or individually ($p < 0.001$) (Fig. 3C). Glutamate uptake experiments were performed in a similar manner on HEK^+ cells. As observed in $MSCs^+$, HEK^+ cells showed a specific [^{3}H]glutamate uptake with a similar EC_{50} (62 μM) as that determined for $MSCs^+$. No specific [^{3}H]glutamate uptake was observed in HEK^- cells (Fig. 3D). [^{3}H]glutamate uptake into HEK^+ cells was blocked when $EAAT_2$ inhibitors (TBOA and DHK) were added together (Fig. 3E) or separately ($p < 0.001$) (Fig. 3F).

3.3. Phenotype evaluation of $MSCs^+$

Some of the most important characteristics contributing to the beneficial effects of MSCs in stroke are their angiogenic properties, as well as their capability to act as a source of growth factors and cytokines [32]. Here, we evaluated whether $EAAT_2$ expression modified the intrinsic characteristics of $MSCs^+$ and determined their angiogenic capacity, their capacity to secrete VEG, and the expression of membrane mesenchymal markers ($CD90^+$, $CD73^+$, and $CD45^-$).

The angiogenic capacity of $MSCs^+$ was examined by an *in vitro* matrigel tube formation assay, confirming that the number of rings identified was similar to those obtained with $MSCs^-$ (Fig. 4A–C). The release of VEGF by $MSCs^+$ and $MSCs^-$ was also similar (Fig. 4D). The analysis of membrane mesenchymal phenotype markers ($CD90^+$, $CD73^+$, and $CD45^-$) was performed by flow cytometry, which showed that $MSCs^+$ and $MSCs^-$ did not differ in surface marker expression (Fig. 4E).

3.4. Animals included in the study

Once the expression and functionality of $EAAT_2$ was evaluated in $MSCs^+$ and HEK^+ cells, their blood glutamate-grabbing activity was analyzed first in healthy animals and then in ischemic animal models. A total of 179 experimental animals (male Wistar rats) were used in this study. Forty-eight rats were used to study the effect of $MSCs^+$ and HEK^+ cells on blood glutamate-grabbing, and the remaining 131 were used in the ischemic study. From these, 72 rats were excluded because they did not meet the inclusion criteria and 11 died; finally, 48 ischemic rats were examined (Fig. S6).

3.5. Analysis of blood glutamate concentration in healthy animals treated with $MSCs^+$ and HEK^+ cells

To evaluate the effect of $MSCs^+$ and HEK^+ cells on blood glutamate reduction in healthy animals, a cell dose/response study was performed with i.v. administered 1×10^6, 2×10^6, and 3×10^6 cells/animal. A dose of 3×10^6 cells/animal was necessary to obtain a reduction in glutamate levels (Fig. 5A). Then, eight experimental groups were designed to compare the efficacy of the cells' glutamate-grabbing therapy on glutamate reduction with respect to oxaloacetate treatment. These groups were as follows: (i) a control group treated with saline (vehicle), (ii) a group treated with oxaloacetate (35 mg/kg) [13] used as a positive control for blood glutamate reduction, (iii) a group treated with 3×10^6 HEK^- cells, (iv) a group treated with 3×10^6 HEK^+ cells, (v, vi) two groups treated with 3 × and 9×10^6 $MSCs^-$, and (vii, viii) two groups treated with 3× and 9×10^6 $MSCs^+$. Glutamate levels were determined before cell administration (*i.e.*, basal levels) and 1, 3, and 4 h after cell administration. All treatments were administered by i.v. bolus in 1 mL of saline.

$MSCs^+$ for animal treatment were taken 48 h after transfection (see Fig. 1B). HEK^+ cells were taken from the stably transfected cell clone (see Fig. 2D). Blood glutamate concentrations in animals treated with saline did not change significantly within the first 4 h after treatment. Similarly, the groups of animals treated with non-transfected cells—HEK^- and $MSCs^-$—did not show a significant reduction in blood glutamate levels after treatment administration either. In line with our previous results [13], oxaloacetate led to a reduction in glutamate at 1 h ($p < 0.05$) and 4 h ($p < 0.05$) after the administration of the compound. The administration of 3×10^6 HEK^+ cells resulted in a reduction in blood glutamate levels 1 and 3 h after injection. With 3×10^6 $MSCs^+$, a significant glutamate reduction was measured 1 and 2 h after cell administration ($p < 0.05$, $n = 6$/group) (Fig. 5B). A higher dose of $MSCs^+$ (9×10^6) did not increase the reduction in blood glutamate levels compared to the values achieved with 3×10^6 $MSCs^+$; however, the effect lasted longer and was detectable even 4 h after cell administration. Notably, the treatment of rats with $MSCs^+$ reduced the blood glutamate to a level similar to that measured 4 h after oxaloacetate administration.

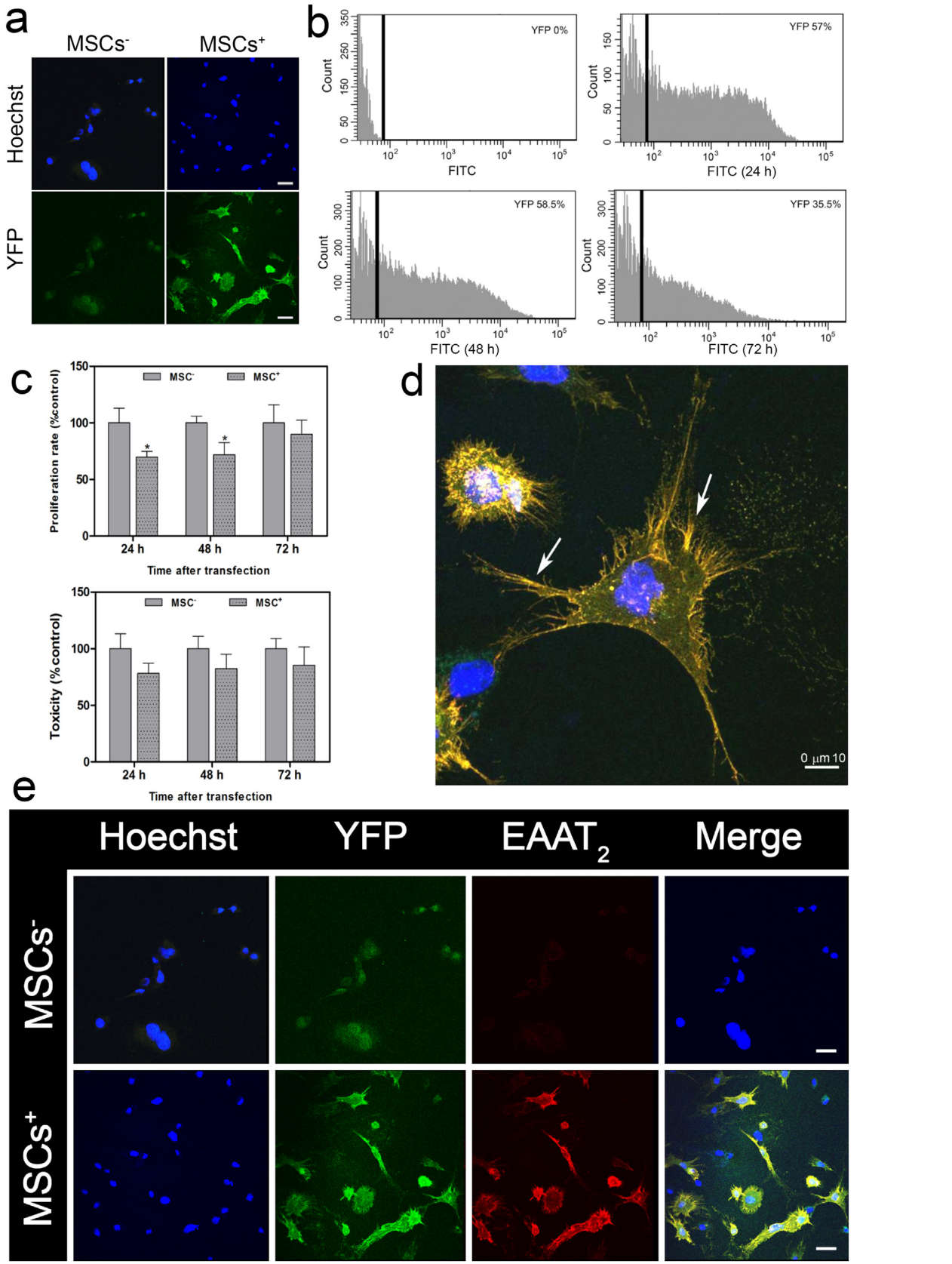

Fig. 1. Analysis of YFP-EAAT$_2$ expression in MSCs. (A) Confocal image of control (MSCs$^-$) and YFP-EAAT$_2$-expressing MSCs (MSCs$^+$) after electroporation (scale bar, 25 µm). (B) YFP fluorescence in MSCs analyzed by flow cytometry: non-transfected cells (FITC) and transfected cells (FITC 24 h, FITC 48 h, and FITC 72 h) after transfection. (C) Analysis of the proliferation rate and toxicity (measured by an LDH assay) of electroporated cells without plasmid (MSCs$^-$) and with the YFP-EAAT$_2$-encoding construct (MSCs$^+$). Data shown are normalized to MSC$^-$ levels (*$p < 0.05$, $n = 3$). (D) Immunocolocalization of YFP-EAAT2 in MSCs$^+$ (scale bar, 10 µm). (E) Immunofluorescent labeling of nuclei (Hoechst, blue), YFP (green), and EAAT2 (red) in control (MSCs$^-$) and transfected MSCs$^+$ (scale bar, 25 µm).

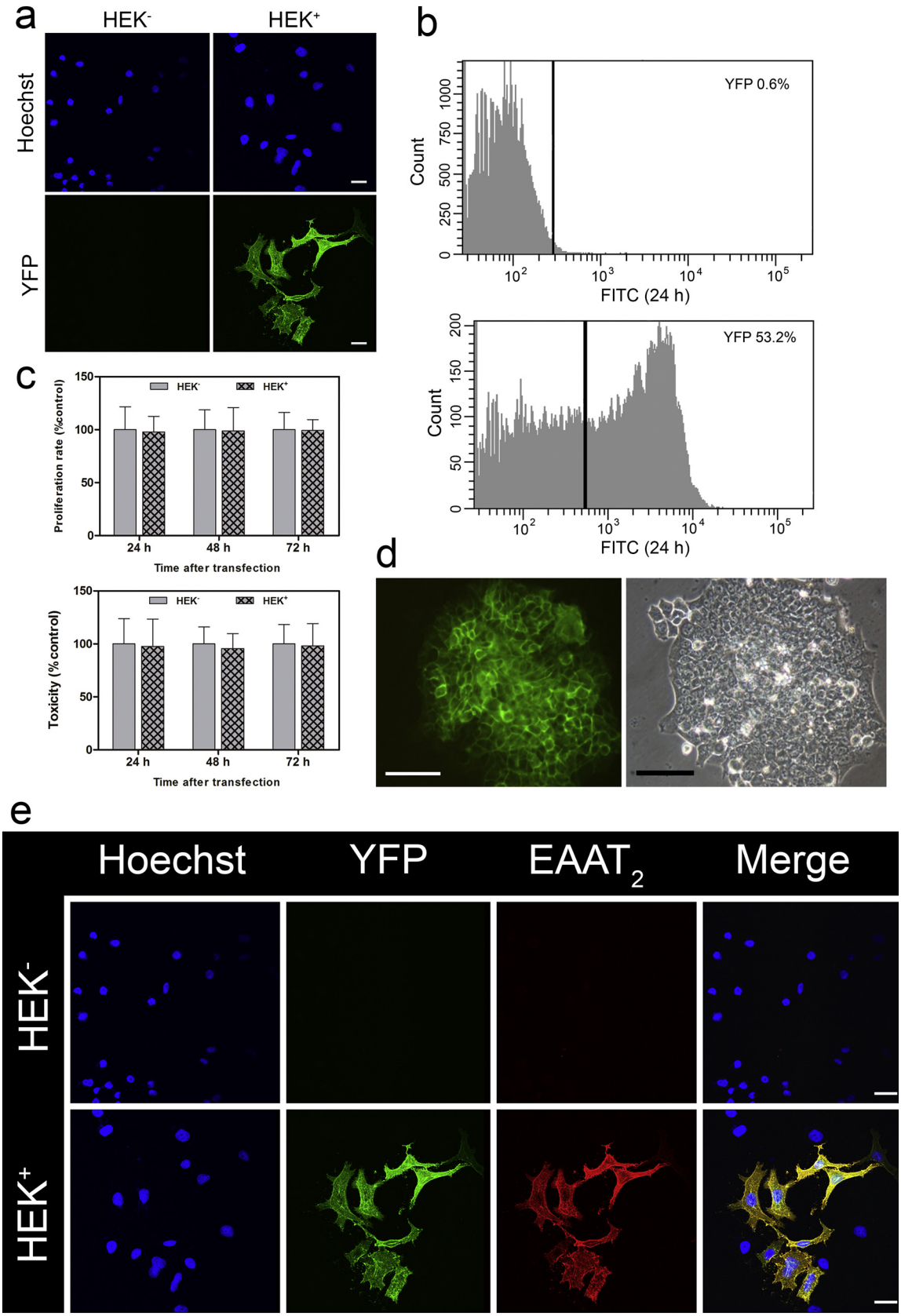

Fig. 2. Analysis of YFP-$EAAT_2$ expression in HEK cells. (A) Confocal image of YFP-$EAAT_2$-expressing HEK cells after calcium phosphate transfection (scale bar, 25 μm). (B) YFP fluorescence in HEK cells analyzed by flow cytometry: before and 48 h after transfection. (C) Analysis of proliferation rate and toxicity (measured by an LDH assay). Data are normalized to HEK^- levels ($^*p < 0.05$, n = 3). (D) An HEK^+ colony constitutively expressing YFP-$EAAT_2$ (scale bar, 100 μm). (E) Immunofluorescent labeling of nuclei (Hoechst, blue), YFP (green), and $EAAT_2$ (red). Scale bar, 25 μm. Non-transfected HEK cells (HEK^-); transfected HEK cells (HEK^+).

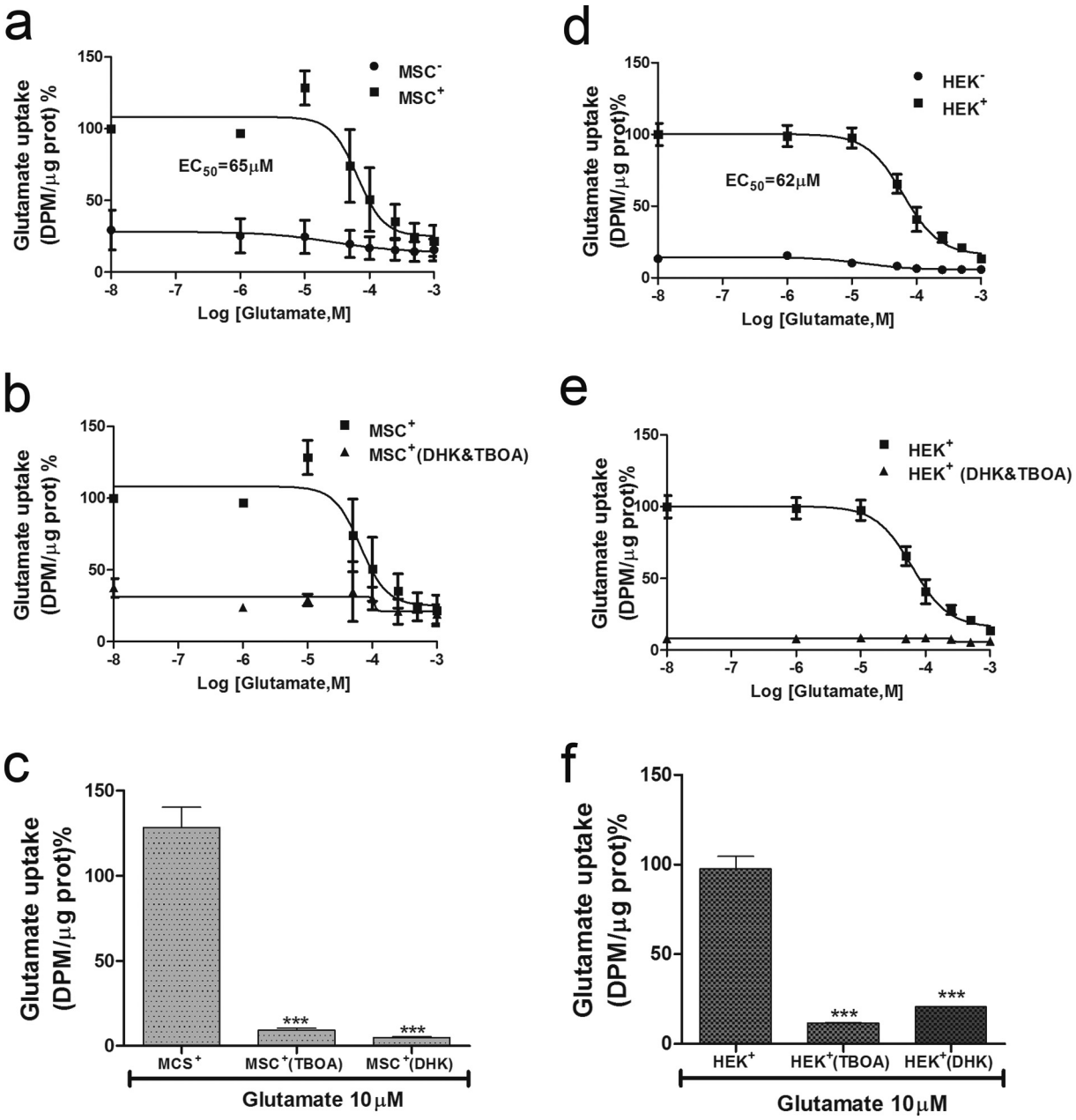

Fig. 3. Evaluation of glutamate uptake in MSCs$^+$ and MSCs. (A) [^{3}H]glutamate uptake in MSCs$^+$ and MSCs in the presence of increasing concentrations of non-labeled glutamate. (B) Inhibition of [^{3}H]glutamate uptake mediated by the simultaneous application of DHK (300 μM) and TBOA (500 μM) in MSCs$^+$. (C) Inhibition of [^{3}H]glutamate uptake with both inhibitors applied individually to MSCs$^+$ (***$p < 0.001$, $n = 6$). (D) [^{3}H]glutamate uptake assay in HEK$^+$ and HEK$^-$ cells. (E) Selective inhibition of glutamate uptake mediated by the simultaneous application of DHK and TBOA in HEK$^+$ cells, and (F) inhibition of glutamate uptake with both inhibitors administered individually to HEK$^+$ cells (***$p < 0.001$, $n = 6$). Radioactive disintegrations per minute (DPM); protein (prot); DL-threo-beta-benzyloxyaspartate (TBOA); dihydrokainate (DHK); non-transfected MSCs (MSC$^-$); transfected MSCs (MSC$^+$).

3.6. Comparative protective effect of MSCs$^+$ and HEK$^+$ cells against oxaloacetate treatment in ischemic animal models

Once the blood glutamate-grabbing efficacy in healthy rats was evaluated, the protective effect of MSCs$^+$ and HEK$^+$ cells was tested in ischemic rat models. No effect on blood glutamate reduction was observed in the rats treated with saline and non-transfected cells (3×10^6 HEK$^-$, 3×10^6 MSCs$^-$, and 9×10^6 MSCs$^-$). Ischemic rats treated with oxaloacetate and 3×10^6 HEK$^+$ cells showed significant reductions ($p < 0.05$, $n = 6$/group) in blood glutamate levels 1 h after treatment. The effect lasted even longer (3–4 h) when 3×10^6 or 9×10^6 MSCs$^+$ were administered (Fig. 6A).

MRI analysis during the occlusion revealed that all animals showed similar ischemic lesions before the administration of cells or oxaloacetate (average ischemic lesion, 42% ± 4%, adjusted to the ipsilateral hemisphere). Inspection of the infarct volume on day 14 showed that oxaloacetate, 3×10^6 MSCs$^+$, and interestingly, 3×10^6 and 9×10^6 of both MSC$^-$-treated groups showed reductions in infarct volume (30.9% ± 5% *vs.* 24.3% ± 4%; 30.9% ± 5% *vs.* 25.4% ± 3%; 30.9% ± 5% *vs.* 22.7% ± 3%, and 30.9% ± 5% *vs.* 13.5% ± 11%; respectively, $p < 0.05$, $n = 6$/group). A trend of reduced infarct volume was also observed with 9×10^6 MSCs$^+$, but this effect was not statistically significant (Fig. 6B and C). Associated with the regression of the infarct volume, a functional recovery of the rats occurred, which was examined by the cylinder test. Notably, the administration of 3×10^6 HEK$^+$ cells also resulted in functional improvement (Fig. 6D).

Histological analysis of a neuronal marker (NeuN) and a glial marker (GFAP) performed 14 days after lesioning did not reveal expression

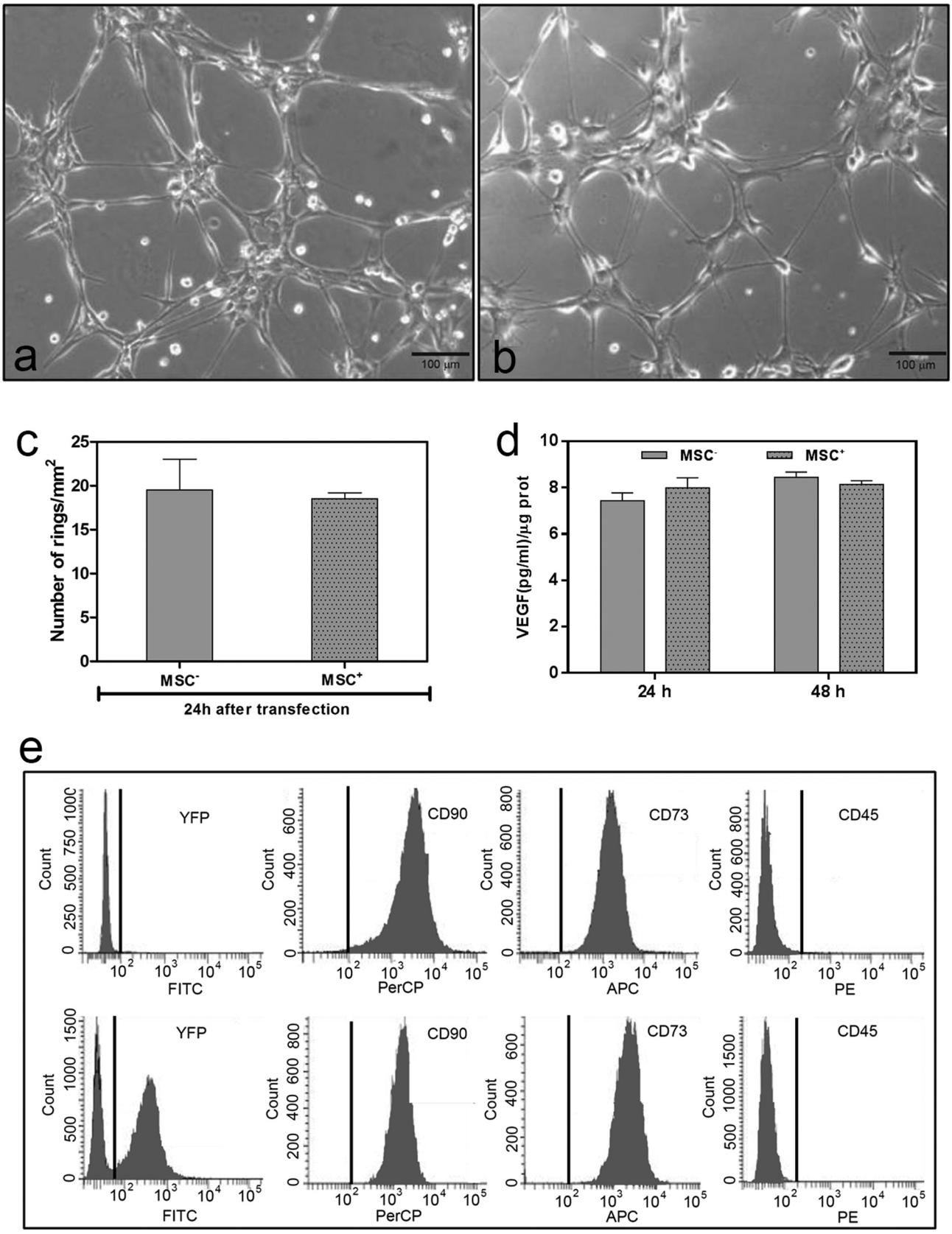

Fig. 4. Examination of MSC characteristics. Phase-contrast image of matrigel angiogenic assay in MSCs^{-} (A) and MSCs^{+} (B), (scale bar, 100 μm). (C) Analysis of ring formation of MSCs^{-} and MSCs^{+}. Data are shown as mean ± SD ($n = 3$). (D) VEGF release determined at different time-points in MSCs^{-} and MSCs^{+}. Data are shown as mean ± SD (n = 3). (E) Analysis of mesenchymal phenotype markers (CD90^{+}, CD73^{+}, and CD45^{-}) in MSCs^{-} (upper panel) and MSCs^{+} (lower panel) by flow cytometry (n = 3). Non-transfected MSCs (MSC^{-}), transfected MSCs (MSC^{+}), fluorescein isothiocyanate (FITC), allophycocyanin (APC), peridinin chlorophyll protein c complex (PerCP), phycoerythrin (PE), yellow fluorescent protein (YFP).

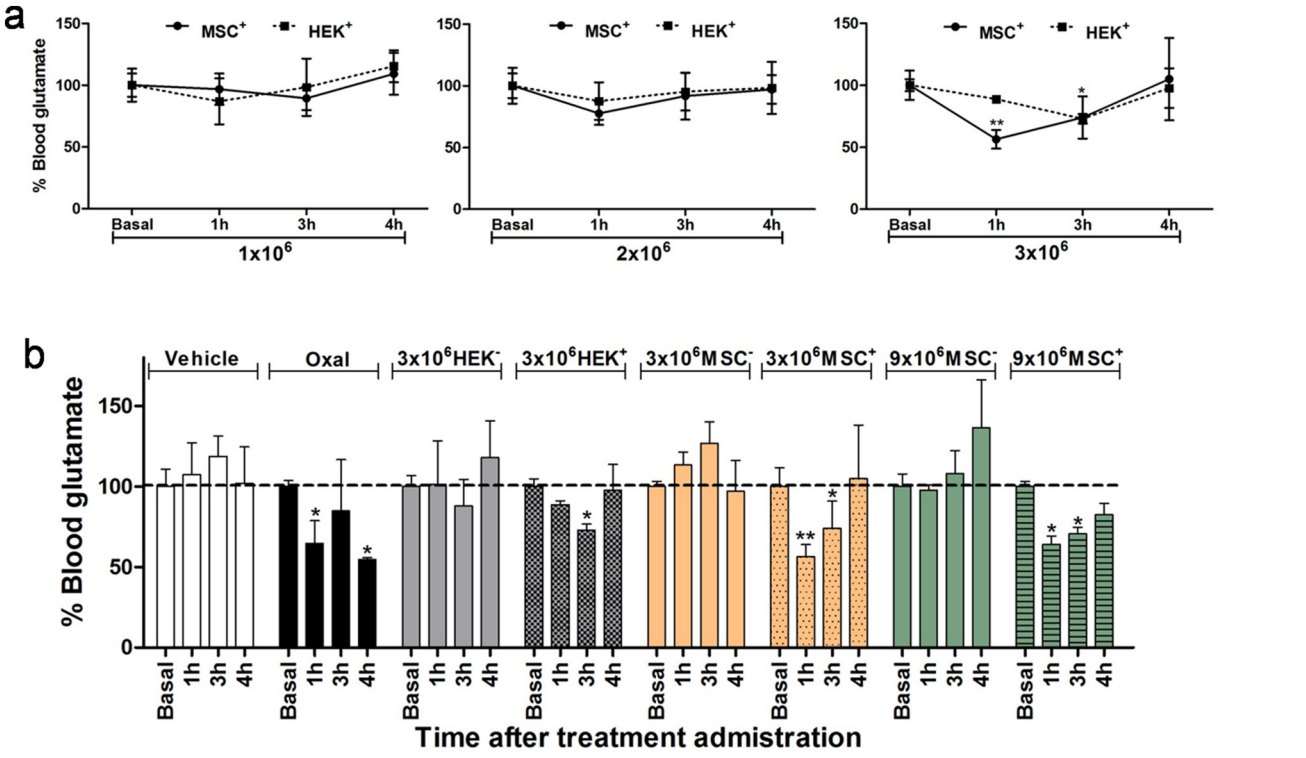

Fig. 5. Analysis of cell glutamate in healthy rats. (A) Dose/response analyses of 1×10^6, 2×10^6, and 3×10^6 HEK^+ cells and $MSCs^+$/animal on blood glutamate levels 4 h after cell administration. (B) Effect of the different treatments on blood glutamate concentration at distinct time-points in healthy animals. Data are normalized to basal glutamate levels (*$p < 0.05$, **$p < 0.01$, $n = 6$/group). The dashed line represents the 100% value of basal glutamate levels. Non-transfected MSCs (MSC^-); transfected MSCs (MSC^+); non-transfected HEK cells (HEK^-); transfected HEK cells (HEK^+).

differences in either antigen in the striatum of the ischemic side among any experimental group (Fig. S7). Interestingly, in the cortical region (Fig. 6E), a higher (although not significant) neuronal survival rate and smaller lesion scar were found in the groups treated with oxaloacetate, 3×10^6 $MSCs^-$/$MSCs^+$, and 9×10^6 $MSCs^-$, *i.e.*, where the infarct volume had also significantly regressed during the observation period of 14 days (Fig. 6F and G).

3.7. $EAAT_2$ expression in MSCs is associated with the release of IL-6

In an attempt to explain the lower protective effect of $MSCs^+$ than that of $MSCs^-$ in ischemic animals, we examined whether the transfection procedure could affect the release of IL-6, one of the most representative cytokines associated with the immunomodulatory function of MSCs [25,33,34].

Analysis of IL-6 levels in the supernatants of MSC^- and MSC^+ cultures 24 h after electroporation showed an increase in IL-6, from 2.0 ± 0.2 pg/mL to 32.9 ± 8.5 pg/mL and 35.3 ± 9.5 pg/mL ($p < 0.05$) in $MSCs^+$ and $MSCs^-$, respectively, whereas no change in IL-6 secretion was detected in MSCs that had not been electroporated (MSCs). Cells electroporated with a control plasmid also showed a release of IL-6 (2.5 ± 0.3 *vs.* 63.1 ± 8.5 pg/mL ($p < 0.05$).

Stimulation of non-electroporated MSCs and electroporated MSCs with LPS, a proinflammatory agent, confirmed the intrinsic capacity of MSCs to release IL-6 in response not only to mechanical stress (as electroporation) but also to pro-inflammatory stimuli (Fig. 7A).

Analysis of IL-6 in blood samples from ischemic rats before (basal) and after treatment with saline (vehicle) and 9×10^6 $MSCs^-$ showed increased IL-6 levels 24 h after ischemia regardless of whether vehicle or cells were administered (vehicle: 7.5 ± 13 pg/mL *vs.* 45.6 ± 23 pg/mL; $MSCs^-$: 4.8 ± 15 pg/mL *vs.* 27.2 ± 23 pg/mL, $p < 0.05$, Fig. 7B). However, in line with the *in vitro* analysis (Fig. 7A), this increase was significantly higher in rats treated with 9×10^6 transfected cells ($MSCs^+$: 3.8 ± 6 pg/mL *vs.* 89.0 ± 9 pg/mL; $p < 0.05$, Fig. 7B).

4. Discussion

Blood/brain glutamate-grabbing is an emerging protective strategy to reduce the excitotoxic effect of the elevated extracellular glutamate that accumulates in the brain during the acute phase of ischemic stroke [9,18]. This novel protective strategy has been tested by several laboratories in different ischemic animal models [13,16,35–38], using the two most common pharmacological approaches, *i.e.*, oxaloacetate and rGOT1 application. The protective mechanism has also been validated by non-pharmacological approaches like peritoneal dialysis, used to filter the blood and remove excess glutamate [19,39,40]. All these studies imply that blood glutamate reduction holds great potential as an effective protective strategy to reduce the neurotoxic increase in glutamate in the brain. On the basis of the high specificity of excitatory amino acid transporters, *e.g.*, $EAAT_2$, for glutamate uptake, we developed a novel cell-based blood/glutamate-scavenging approach by introducing the coding sequence of $EAAT_2$ into MSCs, combining the intrinsic properties of these cells with excitotoxic protection. Here, we compared the blood glutamate-grabbing efficacy of this cell-based strategy with the "gold standard," *i.e.*, oxaloacetate treatment.

The transporter was successfully expressed in MSCs and HEK 293 cells. In both cell types, the expression of YFP-$EAAT_2$ was confirmed by immunological staining and flow cytometry. The functionality of the transporter was determined by [^{3}H]glutamate uptake assays, and the blood glutamate-grabbing activity was validated in healthy rats. The results demonstrated that systemic administration of cells expressing $EAAT_2$ significantly reduces blood glutamate levels. The effect on blood glutamate reduction produced by $MSCs^+$ and HEK^+ was very similar to that resulting from oxaloacetate administration. The highest dose of $MSCs^+$ (9×10^6 cells) reduced the glutamate concentration for up to

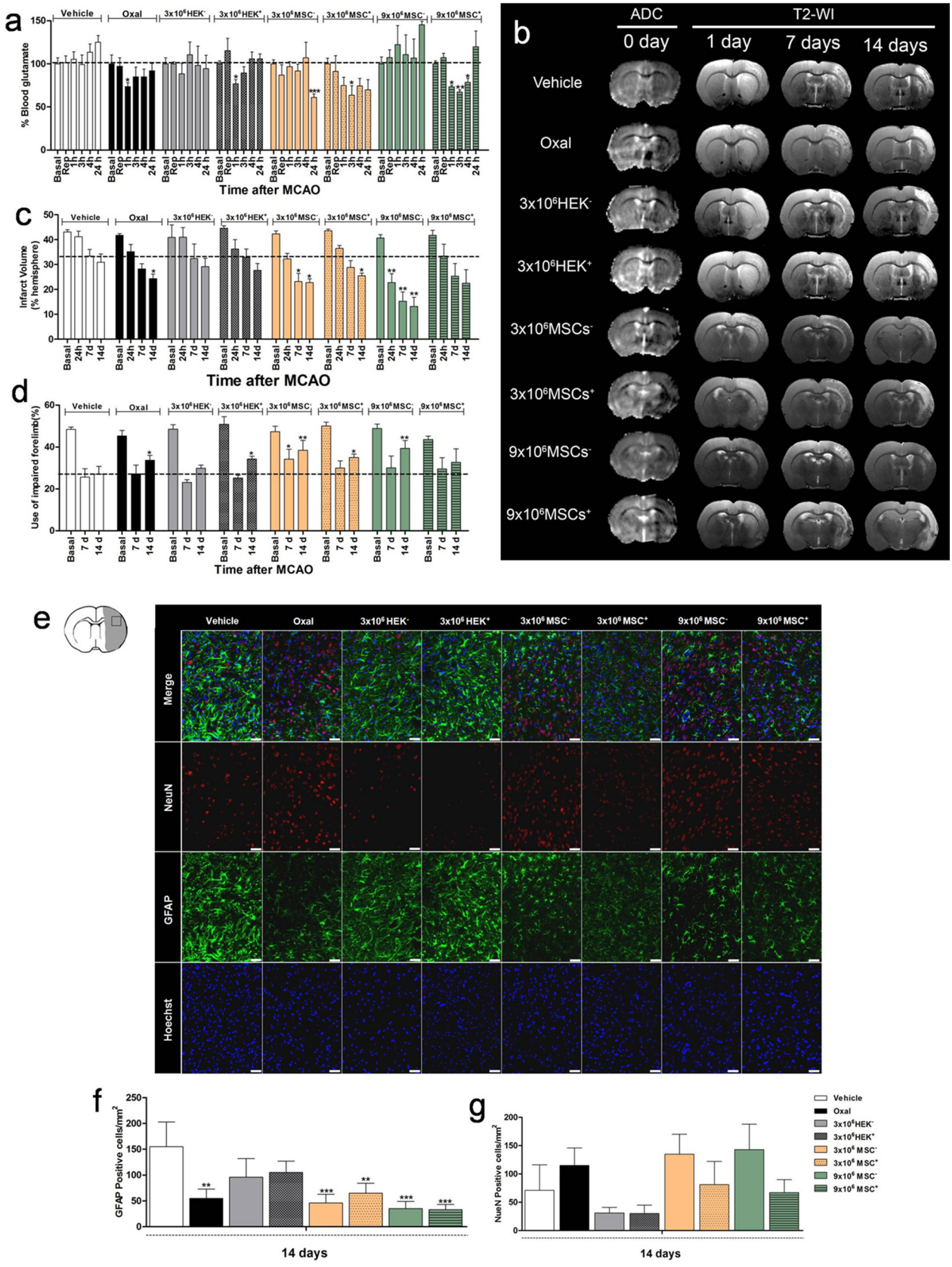
a
Vehicle
Oxal
3x10⁶HEK⁻
3x10⁶HEK⁺
3x10⁶MSC⁻
3x10⁶MSC⁺
9x10⁶MSC⁻
9x10⁶MSC⁺
% Blood glutamate
Basal
Rep
1h
3h
4h
24 h
Time after MCAO
b
ADC
T2-WI
0 day
1 day
7 days
14 days
Vehicle
Oxal
3x10⁶HEK⁻
3x10⁶HEK⁺
3x10⁶MSCs⁻
3x10⁶MSCs⁺
9x10⁶MSCs⁻
9x10⁶MSCs⁺
c
Infarct Volume (% hemisphere)
Basal
24h
7d
14d
Time after MCAO
d
Use of impaired forelimb(%)
Basal
7 d
14 d
Time after MCAO
e
Vehicle
Oxal
3x10⁶ HEK⁻
3x10⁶ HEK⁺
3x10⁶ MSC⁻
3x10⁶ MSC⁺
9x10⁶ MSC⁻
9x10⁶ MSC⁺
Merge
NeuN
GFAP
Hoechst
f
GFAP Positive cells/mm²
14 days
g
NueN Positive cells/mm²
14 days
Vehicle
Oxal
3x10⁶HEK⁻
3x10⁶HEK⁺
3x10⁶ MSC⁻
3x10⁶ MSC⁺
9x10⁶ MSC⁻
9x10⁶ MSC⁺

4 h; yet, the absolute reduction was not higher than that with 3×10^6 cells or oxaloacetate. It is tempting to speculate that a higher expression level of $EAAT_2$ or higher cell doses per animal could increase the glutamate-grabbing efficacy. Here, as well as in previous studies [26,27], the expression of $EAAT_2$ in $MSCs^+$ and HEK^+ cells was technically optimized to gain high transporter levels per cell and simultaneously keep the cells healthy. We are aware that alternative strategies, *e.g.*, invoking lentivirus infection, may result in even higher transduction rates, and this aspect should be addressed in forthcoming studies. Regarding the cell dose used, we established 3×10^6 cells per animal as a threshold necessary to induce a significant reduction in blood glutamate levels. The risk of cell aggregation and pulmonary embolism has been described in other studies [41]; therefore, to avoid the death of the animals, doses higher than 9×10^6 $MSCs^+$ were not used. Owing to the lack of experience and literature on HEK cells for i.v. administration and to reduce the risk of systemic embolisms, doses higher than 3×10^6 cells were not tested.

The therapeutic effect of $MSCs^+$ and HEK^+ cells was thoroughly examined in ischemic rats and compared with that of oxaloacetate treatment. In line with the results in healthy rats, the administration of transfected cells and oxaloacetate significantly reduced blood glutamate levels, which was associated with the functional recovery of the animals. However, oxaloacetate, 3×10^6 $MSCs^+$, and surprisingly, $MSCs^-$ (3×10^6 and 9×10^6 cell doses) were the only treatments that dually caused functional recovery and a reduction in infarct volume.

HEK 293 cells are widely used in *in vitro* cell studies because they are easy to handle, grow rapidly, are resistant to stressful conditions, and can be readily transfected [42]. Therefore, this cell line represented an excellent model to test the effect of $EAAT_2$ cell expression on blood glutamate reduction. The functional improvement observed in ischemic animals treated with HEK^+ cells confirmed that this effect was indeed mediated by the glutamate-grabbing activity associated with $EAAT_2$ functionality.

The administration of HEK^+ cells and oxaloacetate in ischemic animals resulted in almost similar glutamate reductions. However, the protective effect was quite different. This suggests that, in addition to the obvious blood glutamate-grabbing effect, oxaloacetate may induce a pleiotropic mechanism protecting the animal against ischemic stroke. Oxaloacetate has been shown to serve as an antioxidant when cells are subjected to stressful stimuli, such as hydrogen peroxide, thiobarbituric acid reactive species, or excitotoxic damage [15].

MSCs are currently the most promising candidates for stem cell therapy against ischemic stroke owing to their intrinsic capability to secrete growth factors and immunomodulatory cytokines, which equip these cells with neuroprotective and neurorecovery properties [32]. Therefore, we hypothesized that the addition of a glutamate-grabbing property should increase the protective effect of MSCs against cerebral ischemia. The expression of $EAAT_2$ in MSCs effectively conferred the expected glutamate-grabbing activity validated in healthy and ischemic animals. Unexpectedly, the protective effect observed on infarct volume reduction and functional recovery after MSC^+ administration was not as pronounced as with $MSCs^-$. This finding suggests that the transfection procedure most likely interferes with some of the intrinsic protective mechanisms of mesenchymal cells. We could exclude the effect of the transfection procedure on the release of VEGF and membrane phenotype. The quantification of IL-6 secretion, which is considered one of the most representative cytokines [34], in MSC supernatants revealed that the electroporation procedure rather than plasmid expression induced the release of this cytokine. This might explain the loss of the beneficial effect with $MSCs^+$ that we observed with MSCs. In fact, MSCs electroporated with control plasmids (sham MSCs) were not included as an additional group in the animal study mainly because wanted to compare the behavior of $MSCs^+$ with that of healthy MSCs.

That MSCs release IL-6 upon LPS stimulation or other stressful stimuli like H_2O_2 [43] is well-documented [44]. However, there are conflicting reports on the potential effects of this cytokine in stroke. Some studies have found that the external administration of IL-6 in ischemic animal models leads to an improvement in the animal outcome [45], while we recently reported IL-6 to be associated with poor outcome in a study on 4112 stroke patients [46], a finding that is corroborated by the present findings. We cannot exclude that an alteration in the release of other mesenchymal factors or cytokines could contribute to reduce the beneficial effect of transfected MSCs in ischemic animals. From our study, we can deduce that the experimental manipulation of mesenchymal cells induces an alteration of their intrinsic properties and reduces their beneficial properties, which is an important issue for studies focusing on the therapeutic effects of MSCs.

We previously evaluated the fate and biodistribution of MSCs after i.v. administration in the same ischemic animal model as we have used in this study [30]. We observed that the benefits observed after i.v. delivery of MSCs were not attributable to the cell engraftment in the brain as MSCs did not reach the brain tissue, and positively labeled cells were found to be distributed mainly along the lungs. Therefore, we can assume that the effect of MSCs on glutamate and infarct reduction was mediated by a systemic effect and not the engraftment and dedifferentiation into cerebral $EAAT_2$-expressing cells, as astrocytes or endothelial cells.

This study had some limitations that should be taken into consideration. One of the main limitations of protective drugs against glutamate excitotoxicity after stroke is the narrow therapeutic time window, mainly because the increase in glutamate release appears immediately after stroke; therefore, treatments against glutamate excitotoxicity should be administered as soon as possible but within a clinically relevant time window. In this study, cell infusions were applied upon reperfusion, only 75 min after occlusion onset. This could be considered an early treatment regimen, which might be impractical in the clinic setting. However, although the metabolic rate in rats is faster than that in humans (~6.4 times faster [47]), making the time window clinically acceptable, further studies should determine the time window of these cell therapies.

In summary, our results show that cell-based therapies using the administration of $EAAT_2$-expressing cells to ischemia-lesioned animal models is a novel alternative to reduce glutamate neuronal excitotoxicity. Although further studies are necessary to optimize the $EAAT_2$ expression in mesenchymal cells, this study opens up avenues for combining a protective strategy with a cell therapy for cerebral ischemia.

Fig. 6. $EAAT_2$–cell-based glutamate-grabbing therapy in ischemic rat models. (A) Effect of the different treatments on blood glutamate concentration at different time-points in ischemic animals. Data are shown as % ± SD relative to the basal levels (*$p < 0.05$, **$p < 0.01$ compared with the control group at the same time-point; n = 6/group). The dashed line represents the 100% value of basal glutamate levels. (B) Representative MRI of each experimental group at different time-points. ADC maps were determined during ischemia induction and T_2-weighted imaging at 1, 7, and 14 days. ADC maps were used to determine the basal ischemic lesion before treatment administration. (**C**) Effect of the different treatments on infarct size at different time-points in ischemic animals. Data are shown as % ± SD relative to the ischemic hemisphere (*$p < 0.05$, **$p < 0.01$ compared with the control group at the same time-point; n = 6/group). The dashed line represents the infarct volume at 14 days after surgery of the control group (vehicle). (**D**) Functional analysis determined by the cylinder test at different time-points in ischemic animals. Data are shown as % ± SD compared with the basal group (vehicle) at the same time-point (*$p < 0.05$, **$p < 0.01$; n = 6/group). The dashed line represents the functional deficit of the control group (vehicle) at 14 days after stroke. Non-transfected MSCs ($MSCs^-$), transfected MSCs ($MSCs^+$), non-transfected HEK cells (HEK^-), transfected HEK cells (HEK^+), middle cerebral artery occlusion (MCAO), oxaloacetate (Oxal). (**E**) Histological analysis of neurons (NeuN, red), astrocytes (GFAP, green), and nuclei (Hoechst, blue) of animals from each experimental group at 14 days after ischemic lesion in the cortical region. (**F**) Quantification of GFAP-positive cells/mm^2 and (G) NeuN-positive cells/mm^2 in the cortical ischemic region. Magnification (400×). Scale bar, 50 μm. Data are shown as mean ± SD (n = 3/group). Non-transfected MSCs ($MSCs^-$), transfected MSCs ($MSCs^+$), non-transfected HEK cells (HEK^-), transfected HEK cells (HEK^+), oxaloacetate (Oxal), neurons (NeuN), glial fibrillary acidic protein (GFAP).

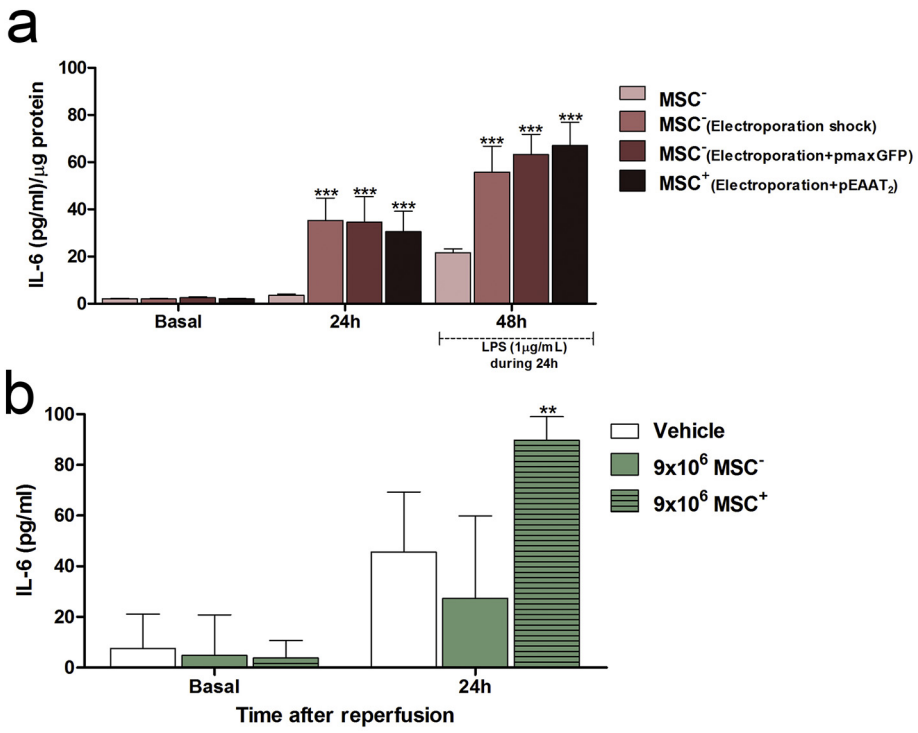

Fig. 7. *In vitro* and *in vivo* determination of the release of IL-6. (A) *In vitro* IL-6 quantities in the supernatants of MSC^{-} and MSC^{+} cultures under basal MSCs is associated with a release of IL-6 conditions 24 h after transfection (with and without plasmid), and 48 h after LPS treatment for 24 h. Data are shown as mean ± SD (***$p < 0.001$, $n = 9$). The plasmid encoding the fluorescent protein eGFP (pmaxGFP) was used as the control. $pEAAT_2$ represents the YFP-$EAAT_2$-encoding construct (B) Serum levels of IL-6 in ischemic rats treated with vehicle, 9×10^6 $MSCs^{-}$, and 9×10^6 $MSCs^{+}$. Data are shown as mean ± SD (**$p < 0.01$, $n = 3$). Non-transfected MSCs ($MSCs^{-}$); transfected MSCs ($MSCs^{+}$); lipopolysaccharide (LPS).

Author contributions

Conception and design of the experiments: M.P-M., J.C., T.S., and F.C. Collection, analysis, and interpretation of data: M.P-M., R.I-R., A.V-P., A. D-L.,B.A., H·F-S., A.S-C., A.P-D., C·C-P., A.G., P.A-G., M.I.L., A.B., J.C., T.S., and F.C. Drafting the article: A.B., J.C., T.S., and F.C. Supervision of the project: J.C. and F.C.

Conflict of interest

The authors declare that no conflict of interest exists.

Acknowledgement

This study was partially supported by grants from Instituto de Salud Carlos III (PI13/00292 and PI17/0054), Spanish Research Network on Cerebrovascular Diseases RETICS-INVICTUS (RD12/0014), Fundación Mutua Madrileña; the Ministry of Economy and Competitiveness of Spain (SAF2014-56336-R), Xunta de Galicia (Programa de Desarrollo Precomercial de los resultados de investigación del Sistema Público de Salud de Galicia_ PRIS); and the European Union program FEDER. Furthermore, F. Campos (CP14/00154) and T. Sobrino (CP12/03121 and CPII17/00027) are recipients of a research contract from Miguel Servet Program of Instituto de Salud Carlos III. Funders had not any role in study design, data collection, data analysis, interpretation, writing of the report.

We thank Prof. C. Fahlke (Institute of Complex Systems – Cellular Biophysics (ICS-4), Forschungszentrum Jülich, Germany) for assistance and for providing the $pRcCMVmYFPEAAT_2$ plasmid.

Appendix A. Supplementary data

Supplementary data to this article can be found online at https://doi.org/10.1016/j.ebiom.2018.11.024.

References

[1] Feigin VL, Forouzanfar MH, Krishnamurthi R, Mensah GA, Connor M, Bennett DA, et al. Global and regional burden of stroke during 1990-2010: findings from the Global Burden of Disease Study 2010. Lancet 2014;383(9913):245–54.
[2] Lai TW, Zhang S, Wang YT. Excitotoxicity and stroke: identifying novel targets for neuroprotection. Prog Neurobiol 2014;115:157–88.
[3] Kim K, Lee SG, Kegelman TP, Su ZZ, Das SK, Dash R, et al. Role of excitatory amino acid transporter-2 (EAAT2) and glutamate in neurodegeneration: opportunities for developing novel therapeutics. J Cell Physiol 2011;226(10):2484–93.
[4] Fahlke C, Kortzak D, Machtens JP. Molecular physiology of EAAT anion channels. Pflugers Archiv 2016;468(3):491–502.
[5] Sheldon AL, Robinson MB. The role of glutamate transporters in neurodegenerative diseases and potential opportunities for intervention. Neurochem Int 2007;51(6–7):333–55.
[6] Leinenweber A, Machtens JP, Begemann B, Fahlke C. Regulation of glial glutamate transporters by C-terminal domains. J Biol Chem 2011;286(3):1927–37.
[7] O'Kane RL, Martinez-Lopez I, Dejoseph MR, Vina JR, Hawkins RA. Na(+)-dependent glutamate transporters (EAAT1, EAAT2, and EAAT3) of the blood-brain barrier. A mechanism for glutamate removal. J Biol Chem 1999;274(45):31891–5.
[8] Cohen-Kashi-Malina K, Cooper I, Teichberg VI. Mechanisms of glutamate efflux at the blood-brain barrier: involvement of glial cells. J Cerebral Blood Flow Metabol 2012;32(1):177–89.
[9] Castillo J, Loza MI, Mirelman D, Brea J, Blanco M, Sobrino T, et al. A novel mechanism of neuroprotection: Blood glutamate grabber. J Cerebral Blood Flow Metabol 2016;36(2):292–301.
[10] Teichberg VI, Cohen-Kashi-Malina K, Cooper I, Zlotnik A. Homeostasis of glutamate in brain fluids: an accelerated brain-to-blood efflux of excess glutamate is produced by blood glutamate scavenging and offers protection from neuropathologies. Neuroscience 2009;158(1):301–8.
[11] Hawkins RA, Vina JR. How glutamate is managed by the blood-brain barrier. Biology 2016;5(4).
[12] Campos F, Rodriguez-Yanez M, Castellanos M, Arias S, Perez-Mato M, Sobrino T, et al. Blood levels of glutamate oxaloacetate transaminase are more strongly associated with good outcome in acute ischaemic stroke than glutamate pyruvate transaminase levels. Clin Sci 2011;121(1):11–7.
[13] Campos F, Sobrino T, Ramos-Cabrer P, Argibay B, Agulla J, Perez-Mato M, et al. Neuroprotection by glutamate oxaloacetate transaminase in ischemic stroke: an experimental study. J Cerebral Blood Flow Metabol 2011;31(6):1378–86.
[14] Campos F, Sobrino T, Ramos-Cabrer P, Castellanos M, Blanco M, Rodriguez-Yanez M, et al. High blood glutamate oxaloacetate transaminase levels are associated with good functional outcome in acute ischemic stroke. J Cerebral Blood Flow Metabol 2011;31(6):1387–93.

[15] Campos F, Sobrino T, Ramos-Cabrer P, Castillo J. Oxaloacetate: a novel neuroprotective for acute ischemic stroke. Int J Biochem Cell Biol 2012;44(2):262–5.
[16] Perez-Mato M, Ramos-Cabrer P, Sobrino T, Blanco M, Ruban A, Mirelman D, et al. Human recombinant glutamate oxaloacetate transaminase 1 (GOT1) supplemented with oxaloacetate induces a protective effect after cerebral ischemia. Cell Death Dis 2014;5:e992.
[17] Zlotnik A, Sinelnikov I, Gruenbaum BF, Gruenbaum SE, Dubilet M, Dubilet E, et al. Effect of glutamate and blood glutamate scavengers oxaloacetate and pyruvate on neurological outcome and pathohistology of the hippocampus after traumatic brain injury in rats. Anesthesiology 2012;116(1):73–83.
[18] da Silva-Candal A, Perez-Diaz A, Santamaria M, Correa-Paz C, Rodriguez-Yanez M, Arda A, et al. Clinical validation of blood/brain glutamate grabbing in acute ischemic stroke. Ann Neurol 2018;84(2):260–73.
[19] Godino Mdel C, Romera VG, Sanchez-Tomero JA, Pacheco J, Canals S, Lerma J, et al. Amelioration of ischemic brain damage by peritoneal dialysis. J Clin Invest 2013;123(10):4359–63.
[20] Boyko M, Gruenbaum SE, Gruenbaum BF, Shapira Y, Zlotnik A. Brain to blood glutamate scavenging as a novel therapeutic modality: a review. J Neural Transm 2014;121(8):971–9.
[21] Boyko M, Melamed I, Gruenbaum BF, Gruenbaum SE, Ohayon S, Leibowitz A, et al. The effect of blood glutamate scavengers oxaloacetate and pyruvate on neurological outcome in a rat model of subarachnoid hemorrhage. Neurotherapeutics 2012;9(3):649–57.
[22] Ruban A, Berkutzki T, Cooper I, Mohar B, Teichberg VI. Blood glutamate scavengers prolong the survival of rats and mice with brain-implanted gliomas. Invest New Drugs 2012;30(6):2226–35.
[23] Ruban A, Malina KC, Cooper I, Graubardt N, Babakin L, Jona G, et al. Combined treatment of an amyotrophic lateral sclerosis rat model with recombinant GOT1 and oxaloacetic acid: a novel neuroprotective treatment. Neurodegener Dis 2015;15(4):233–42.
[24] Zhang D, Mably AJ, Walsh DM, Rowan MJ. Peripheral interventions enhancing brain glutamate homeostasis relieve amyloid beta- and TNFalpha- mediated synaptic plasticity disruption in the rat hippocampus. Cereb Cortex 2017;27(7):3724–35.
[25] Marei HE, Hasan A, Rizzi R, Althani A, Afifi N, Cenciarelli C, et al. Potential of stem cell-based therapy for ischemic stroke. Front Neurol 2018;9:34.
[26] Chicaybam L, Barcelos C, Peixoto B, Carneiro M, Limia CG, Redondo P, et al. An efficient electroporation protocol for the genetic modification of mammalian cells. Front Bioeng Biotechnol 2016;4:99.
[27] Chen C, Okayama H. High-efficiency transformation of mammalian cells by plasmid DNA. Mol Cell Biol 1987;7(8):2745–52.
[28] Chen X, Zhang ZY, Zhou H, Zhou GW. Characterization of mesenchymal stem cells under the stimulation of Toll-like receptor agonists. Dev Growth Differ 2014;56(3):233–44.
[29] Fernandez-Susavila H, Iglesias-Rey R, Dopico-Lopez A, Perez-Mato M, Sobrino T, Castillo J, et al. Inclusion criteria update for the rat intraluminal ischaemic model for preclinical studies. Dis Model Mech 2017;10(12):1433–8.
[30] Argibay B, Trekker J, Himmelreich U, Beiras A, Topete A, Taboada P, et al. Intraarterial route increases the risk of cerebral lesions after mesenchymal cell administration in animal model of ischemia. Sci Rep 2017;7:40758.
[31] Tse DY, Chung I, Wu SM. Pharmacological inhibitions of glutamate transporters EAAT1 and EAAT2 compromise glutamate transport in photoreceptor to ON-bipolar cell synapses. Vision Res 2014;103:49–62.
[32] Hao L, Zou Z, Tian H, Zhang Y, Zhou H, Liu L. Stem cell-based therapies for ischemic stroke. Biomed Res Int 2014;2014:468748.
[33] Gu Y, He M, Zhou X, Liu J, Hou N, Bin T, et al. Endogenous IL-6 of mesenchymal stem cell improves behavioral outcome of hypoxic-ischemic brain damage neonatal rats by supressing apoptosis in astrocyte. Sci Rep 2016;6:18587.
[34] Glenn JD, Whartenby KA. Mesenchymal stem cells: emerging mechanisms of immunomodulation and therapy. World J Stem Cells 2014;6(5):526–39.
[35] Knapp L, Gellert L, Kocsis K, Kis Z, Farkas T, Vecsei L, et al. Neuroprotective effect of oxaloacetate in a focal brain ischemic model in the rat. Cell Mol Neurobiol 2015;35(1):17–22.
[36] Rink C, Gnyawali S, Peterson L, Khanna S. Oxygen-inducible glutamate oxaloacetate transaminase as protective switch transforming neurotoxic glutamate to metabolic fuel during acute ischemic stroke. Antioxid Redox Signal 2011;14(10):1777–85.
[37] Rink C, Gnyawali S, Stewart R, Teplitsky S, Harris H, Roy S, et al. Glutamate oxaloacetate transaminase enables anaplerotic refilling of TCA cycle intermediates in stroke-affected brain. FASEB J 2017;31(4):1709–18.
[38] Nagy D, Marosi M, Kis Z, Farkas T, Rakos G, Vecsei L, et al. Oxaloacetate decreases the infarct size and attenuates the reduction in evoked responses after photothrombotic focal ischemia in the rat cortex. Cell Mol Neurobiol 2009;29(6–7):827–35.
[39] Rogachev B, Ohayon S, Saad A, Vorobiovsky V, Gruenbaum BF, Leibowitz A, et al. The effects of hemodialysis on blood glutamate levels in chronic renal failure: implementation for neuroprotection. J Crit Care 2012;27(6):743.
[40] Rogachev B, Tsesis S, Gruenbaum BF, Gruenbaum SE, Boyko M, Klein M, et al. The effects of peritoneal dialysis on blood glutamate levels: implementation for neuroprotection. J Neurosurg Anesthesiol 2013;25(3):262–6.
[41] He B, Yao Q, Liang Z, Lin J, Xie Y, Li S, et al. The dose of intravenously transplanted bone marrow stromal cells determines the therapeutic effect on vascular remodeling in a rat model of ischemic stroke. Cell Transplant 2016;25(12):2173–85.
[42] Nettleship JE, Watson PJ, Rahman-Huq N, Fairall L, Posner MG, Upadhyay A, et al. Transient expression in HEK 293 cells: an alternative to *E. coli* for the production of secreted and intracellular mammalian proteins. Methods Mol Biol 2015;1258:209–22.
[43] Zhang J, Chen GH, Wang YW, Zhao J, Duan HF, Liao LM, et al. Hydrogen peroxide preconditioning enhances the therapeutic efficacy of Wharton's Jelly mesenchymal stem cells after myocardial infarction. Chin Med J (Engl) 2012;125(19):3472–8.
[44] van den Berk LC, Jansen BJ, Siebers-Vermeulen KG, Roelofs H, Figdor CG, Adema GJ, et al. Mesenchymal stem cells respond to TNF but do not produce TNF. J Leukoc Biol 2010;87(2):283–9.
[45] Gronhoj MH, Clausen BH, Fenger CD, Lambertsen KL, Finsen B. Beneficial potential of intravenously administered IL-6 in improving outcome after murine experimental stroke. Brain Behav Immun 2017;65:296–311.
[46] Bustamante A, Sobrino T, Giralt D, Garcia-Berrocoso T, Llombart V, Ugarriza I, et al. Prognostic value of blood interleukin-6 in the prediction of functional outcome after stroke: a systematic review and meta-analysis. J Neuroimmunol 2014;274(1–2):215–24.
[47] Agoston DV. How to translate time? the temporal aspect of human and rodent biology. Front Neurol 2017;8:92.